MOF-Beads containing inorganic nanoparticles for the simultaneous removal of multiple heavy metals from water

Gerard Boix,[†] Javier Troyano,[†] Luis Garzón-Tovar,[†] Ceren Camur,[†] Natalia Bermejo,[†] Amirali Yazdi,[†] Jordi Piella,[†] Neus G. Bastus,[†] Victor F. Puntes,[†,‡] Inhar Imaz*[†] and Daniel Maspoch*[†,‡]

†*Catalan Institute of Nanoscience and Nanotechnology (ICN2), CSIC and The Barcelona Institute of Science and Technology, Campus UAB, Bellaterra, 08193, Barcelona, Spain.*

‡*ICREA, Pg. Lluis Companys 23, 08010, Barcelona, Spain*

KEYWORDS: *Metal-Organic Frameworks, Composite, Inorganic Nanoparticles, Metal removal, Water treatment.*

ABSTRACT: Pollution of water with heavy metals is a global environmental problem whose impact is especially severe in developing countries. Among water-purification methods, adsorption of heavy metals has proven to be simple, versatile and cost-effective. However, there is still a need to develop adsorbents with a capacity to remove multiple metal pollutants from the same water sample. Herein we report the complementary adsorption capacities of metal-organic frameworks (MOFs; here, UiO-66 and UiO-66$(SH)_2$) and inorganic nanoparticles (iNPs; here, cerium-oxide NPs) into composite materials. These adsorbents, which are spherical microbeads generated in one step by continuous-flow spray-drying, efficiently and simultaneously remove multiple heavy metals from water, including As(III and V), Cd(II), Cr(III and VI), Cu(II), Pb(II) and Hg(II). We further show that these microbeads can be used as packing material in a prototype of a continuous-flow water treatment system, in which they retain their metal-removal capacities upon regeneration with a gentle acidic treatment. As proof-of-concept, we evaluated these adsorbents for purification of laboratory water samples prepared to independently recapitulate each of two strongly-polluted rivers: the Bone (Indonesia) and Buringanga (Bangladesh) rivers. In both cases, our microbeads reduced the levels of all the metal contaminants to below the corresponding permissible limits established by the World Health Organization (WHO). Moreover, we demonstrated the capacity of these microbeads to lower levels of Cr(VI) in a water sample collected from the Sarno River (Italy). Finally, to create adsorbents that could be magnetically recovered following their use in water purification, we extended our spray-drying technique to simultaneously incorporate two types of iNPs (CeO_2 and Fe_3O_4) into UiO-66$(SH)_2$, obtaining CeO_2/Fe_3O_4@UiO-66-$(SH)_2$ microbeads that adsorb heavy metals and are magnetically responsive.

INTRODUCTION

Water pollution is a principal cause of health disorders worldwide.[1–3] Increasing industrial activity, especially in developing countries, often involves contamination of water with soluble toxic metal-ion pollutants that readily accumulate in humans and animals.[3,4] Exposure to heavy metals such as arsenic, cadmium, chromium, lead and mercury, even at trace levels, is especially pernicious to human health.[5,6] Consequently, major efforts have been devoted to the development of water-treatment methods. Recently proposed strategies for wastewater purification include coagulation, filtration and chemical precipitation. However, these methods usually require complex instruments and large facilities, which in turn translate to high maintenance costs. Additionally, they have limited utility for removing pollutants at low concentrations and therefore, must often be combined with complementary methods.

One promising approach for water treatment is adsorption, which has been lauded for its simplicity, versatility, cost efficiency and effectiveness.[7–9] Common adsorbents such as activated carbon, zeolites, clay minerals and natural fibers have been studied for the adsorptive removal of heavy metal ions. However, these materials suffer from drawbacks such as limited regeneration, slow sorption kinetics, relatively low thermal or chemical stability, and limited selectivity.[10,11] Adsorbents for water purification must be able to simultaneously remove co-existing pollutants. Accordingly, they should remove as many different harmful metal ions as possible.[12] An interesting strategy to develop such adsorbents is to combine different adsorbent materials, each with its respective functionality, into a single composite that shows broad-spectrum activity.

Metal-organic frameworks (MOFs), which are porous ordered structures exhibiting large specific surface areas, have recently garnered much attention as adsorbent materials, given their high adsorption capacity and chemical/structural tunability.[13–18] An exemplary case of tunable MOFs is that of the water-stable, zirconium-based, UiO-66 family, which, at their inorganic nodes or organic linkers, can be functionalized with moieties that strongly bind heavy-metal ions. For example, bare UiO-66 has been reported to remove Cr(VI) and As(V) from water, demonstrating adsorption capacities of 86 mg/g and 303 mg/g, respectively.[10,19] Moreover, once functionalized with thiourea groups, this MOF can adsorb various other metal ions, including As(V) (303 mg/g), Hg(II) (769 mg/g), Pb(II) (232 mg/g), Cr(III) (117 mg/g) and Cd(II) (49 mg/g).[10,20] Similarly, functionalization of UiO-66 with thiol groups enhances uptake of Hg(II), even in strongly acidic aqueous solutions and vapors,[21] up to 236 mg/g and increases adsorption of As(III) up to 40 mg/g.[22]

Another class of material that has been widely studied as adsorbents is inorganic nanoparticles (iNPs), which exhibit high activity and specificity towards heavy-metal ions.[23,24] For example, cerium oxide (CeO_2) NPs have exhibited excellent adsorption capacities for the following metal ions in water: Pb(II) (128 mg/g), Cr(VI) (122 mg/g), Cd(II) (93 mg/g) and As(V) (17 mg/g).[25–27] Importantly, some iNPs can be easily magnetically retrieved from solution, thus obviating impractical alternatives such as filtering. However, a drawback of iNPs is their tendency to aggregate, which significantly compromises their adsorption efficiency.

One way to mitigate the iNP-aggregation problem is to incorporate iNPs into the porous matrices of other materials.[28] Among porous materials, MOFs have surfaced as an attractive partner for iNPs, not only to prevent iNP-aggregation and to facilitate their recovery after adsorption process, but also for their remediation capabilities. To date, most MOF/iNP composites have been developed for catalysis.[29] However, within the field of pollutant removal, iNPs have been combined with MOFs to yield MOF/iNP adsorbents with added functionalities such as magnetism[30,31] or photocatalytic degradation.[12,32,33]

Herein we report new composite microbeads (hereafter, *iNP@MOF-Beads*) for simultaneous removal of various metals from water, which we obtained by incorporating inorganic nanoparticles (iNPs) into MOFs via a one-step spray-drying process (Fig. 1). As iNPs, we used CeO_2 and as MOFs, we used the water-stable Zr-MOFs UiO-66 or UiO-66-$(SH)_2$. We tested the resultant composite microbeads (CeO_2@UiO-66 and CeO_2@UiO-66-$(SH)_2$) for purification of synthetic river-water samples prepared as mimics of two polluted rivers, and of a real field sample from another polluted river. Furthermore, we evaluated our iNP@MOF-Beads as packing material in fixed-bed, continuous-adsorption columns. Finally, we developed magnetic CeO_2/Fe_3O_4@UiO-66-$(SH)_2$ microbeads by simultaneously incorporating CeO_2 and Fe_3O_4 NPs into UiO-66-$(SH)_2$.

MATERIALS AND METHODS

Zirconium (IV) propoxide solution (70% (w/w)) in 1-propanol; cerium (III) nitrate; sodium meta arsenite; sodium arsenate dibasic heptahydrate; cadmium (II) nitrate tetrahydrate; chromium (III) nitrate nonahydrate; chromium (VI) oxide; copper (II) nitrate hemi(pentahydrate); lead (II) nitrate; mercury (II) chloride; terephthalic acid; phosphoric acid; diethyl 2,5-dihydroxyterephthalate, polyvinylpyrrolidone (PVP, M_w ~ 10,000), 1,4-diazabicyclo[2.2.2]octane; dimethylthiocarbomoyl chloride and hexamethylenetetramine were purchased from Sigma Aldrich. *N,N*-dimethylformamide (DMF), methanol and acetone were purchased from Fisher Scientific. All the reagents were used without further purification. Deionized water, obtained with a Milli-Q® system (18.2 MΩ·cm), was used in all adsorption experiments. Fe_3O_4 nanoparticles (8-nm; 1 g/L) dispersed in an aqueous solution of PVP (1 mg/mL) was purchased from Applied Nanoparticles. 2,5-dimercaptoterephthalic acid was synthesized according to a reported procedure.[34] X-ray powder diffraction (XRPD) patterns were collected on an X'Pert PRO MPDP analytical diffractometer (Panalytical) at 45 kV and 40 mA using CuKα radiation (λ = 1.5419 Å). Nitrogen adsorption and desorption measurements were performed at 77 K using an Autosorb-IQ-AG analyzer (Quantachrome Instruments). Field-emission scanning electron microscopy (FE-SEM) images were collected on a Magellan 400 L scanning electron microscope (FEI) at an acceleration voltage of 5.0 KV and a Quanta 650F scanning electron microscope (FEI) at an acceleration voltage of 20.0 KV, using aluminum as support. Transmission Electron Microscopy (TEM) images and EDX composition profiles were collected on a Tecnai G2 F20 microscope (FEI) at 200 KV. ^{1}H NMR spectra were acquired in a Bruker Avance III 400SB NMR spectrometer. Inductively Coupled Plasma – Optical Emission Spectroscopy (ICP-OES) measurements were performed on an Optima 4300DV (Perkin-Elmer) instrument.

Synthesis of PVP-functionalized CeO_2 nanoparticles

Cerium-oxide nanoparticles were synthesized according to modified published procedures.[35,36] In a typical experiment, equal volumes of aqueous $Ce(NO_3)_3$ (75 mL, 0.04 M) and aqueous hexamethylenetetramine (75 mL, 0.50 M) were mixed at room temperature and the resultant solution was left at 25 °C for 48 hours under mild stirring. CeO_2 nanoparticles were formed by the controlled oxidation of Ce(III) to Ce(IV) under alkaline conditions, which subsequently precipitated in the form of insoluble CeO_2 species. 4 g of PVP in 200 mL of water was added dropwise to a stirring solution of the iNP and the flask was left to rest overnight at room temperature. Then, 800 mL of acetone was added and the solution was left at room temperature for 24 hours without stirring, leading to precipitation of the NPs. The supernatant was removed by decanting and then, the iNPs were washed three times with DMF. Finally, they were redispersed in DMF to afford a colloidal solution of CeO_2 NPs (1 mg/mL). The average size of the synthesized CeO_2 NPs was 12 nm ± 2.5 nm.

Synthesis of 2,5-dimercaptoterephthalic acid

2,5-dimercaptoterephthalic acid was synthesized according to an adapted literature procedure[34]. Briefly, a solution of diethyl 2,5-dihydroxyterephthalate (0.08 mol, 20 g) in 300 mL of degassed DMF was introduced into a 500 mL three-neck round bottom flask under Ar atmosphere and cooled down to 0˚C. Then, 1,4-diazabicyclo[2.2.2]octane (0.31 mol, 35.2 g) was added under magnetic stirring and the solution was left stirring for 10 minutes. Dimethylthiocarbomoyl chloride (0.32 mol, 39 g) was then slowly added to the mixture, the suspension was allowed to warm to room temperature and then, stirred for 24 hours under Ar atmosphere. The product was precipitated out with 500 mL water, filtered and washed extensively with water (yield: 31 g, 95%). The diethyl 2,5-bis[(dimethylcarbamothioyl)oxy]terephthalate obtained was dried and stored under Ar atmosphere. The obtained product (8 mmol, 3.25 g) was heated under Ar atmosphere at 215 ˚C for 1 hour. The resulting brown paste was cooled down to 70 ˚C and dissolved in 100 mL of EtOH. The solution was cooled down to room temperature, gradually affording fine brown crystals. The crystals were filtered off, yielding diethyl 2,5-bis(dimethylthiocarbamoylsulfanyl)terephthalate (2.75 g, yield 85%). A solution of the previously obtained product (6 mmol, 2.6 g) in a degassed 1.3 M solution of KOH in EtOH/H_2O (1:1, 80 mL) was refluxed for 3 hours under Ar atmosphere. The reaction mixture was cooled down to 0 ˚ C and HCl (37% w/w, 30 mL) was added slowly. The precipitated 2,5-dimercaptoterephthalic acid was collected by filtration, washed extensively with water, dried under dynamic vacuum and stored under Ar (1.29 g, yield 93%). ^{1}H-NMR confirmed formation of the desired product (Fig. S1).

Synthesis of UiO-66, CeO_2@UiO-66, UiO-66-$(SH)_2$ and CeO_2@UiO-66-$(SH)_2$

All materials were synthesized by a slightly modified version of a previously reported spray-drying method[37]. Briefly, terephthalic acid (0.6 mmol, 100 mg), glacial acetic acid (3 mL), a solution of CeO_2 NPs in DMF (1 mg/mL; 8.5 mL) and a 70% (w/w) solution of zirconium (IV) propoxide ($Zr(OPr^n)_4$) in 1-propanol (0.5 mmol, 280 µL) were sequentially added to a flask containing 40 mL of DMF. The resulting mixture was injected into a coil-flow reactor (inner diameter: 3 mm) at a feed rate of 2.4 mL/min at 115 ˚C. The resulting pre-heated solution was then spray-dried at 180 ˚C, at a flow rate of 336 mL/min, using a B-290 Mini Spray-Dryer (BUCHI Labortechnik; spray cap hole diameter: 0.5 mm). The resulting solid was dispersed in DMF, washed twice with DMF and ethanol, and finally dried for 12 h at 85 °C under vaccum. Encapsulation efficiency was determined by ICP-OES and was found to be 4.0% w/w (93% encapsulation yield) for the CeO_2@UiO-66 composite. The thiolated materials were synthetized following the same procedure, except that terephthalic acid was replaced with 2,5-dimercaptoterephthalic acid (proportional molar ratio) and plain DMF instead of a CeO_2 NP dispersion, when appropriate. For the CeO_2@UiO-66-$(SH)_2$ composite, the level of encapsulation of CeO_2 iNPs was calculated to be 3.3% w/w (87% encapsulation yield).

Synthesis of CeO_2/Fe_3O_4@UiO-66-$(SH)_2$

This composite was synthesized following the above procedure with minor modifications. Briefly, 2,5-dimercaptoterephthalic acid (0.6 mmol, 138 mg), glacial acetic acid (3 mL), a dispersion of CeO_2 and Fe_3O_4 iNPs in DMF (1 mg/mL of CeO_2 and 2 mg/mL of Fe_3O_4; 8.5 mL) and a 70% (w/w) solution of $Zr(OPr^n)_4$ in 1-propanol (0.5 mmol, 280 µL) were sequentially added to a flask containing 40 mL of DMF. The resulting mixture was spray-dried, and the resultant solid was washed and dried, as above. Encapsulation of the nanoparticles was monitored by TEM imaging and ICP-OES analysis. The encapsulation efficiencies were 3.0% w/w (79% encapsulation yield) for the CeO_2 iNPs and 9.3% w/w (97% encapsulation yield) for the Fe_3O_4 iNPs.

Metal-adsorption studies

Single-metal adsorption

1 mg of UiO-66, CeO_2@UiO-66, UiO-66-$(SH)_2$ or CeO_2@UiO-66-$(SH)_2$ was added to a 50 mL Falcon centrifugation tube containing 30 mL of a 100 ppb aqueous solution (pH 5) of one of the following metal ions: As(III), As(V), Cd(II), Cr(III), Cr(VI), Cu(II), Pb(II) or Hg(II) (*i.e.* each tube corresponded to a single metal). The Falcon tubes were sonicated for 2 minutes to ensure homogeneous dispersion and then, agitated for 3 hours at 30 rpm in a rotary agitator at room temperature. Afterwards, the samples were centrifuged, and the supernatant was collected through a 200 µm syringe filter and finally, stored at 4 ˚C in the dark until ICP-OES analysis.

Multi-metal adsorption

1 mg of CeO_2@UiO-66-$(SH)_2$ was loaded into a 50 mL Falcon centrifugation tube containing 30 mL of a 100 ppb aqueous solution (pH 5) of all of the following metal ions: As(III), As(V), Cd(II), Cr(III), Cr(VI), Cu(II), Pb(II) and Hg(II) (*i.e.* the tube contained all the metals, each at 100 ppb). The rest of the procedure was the same as for the single-pollutant analysis (see above).

Continuous-flow adsorption and regeneration

The packed-powder column prototype was made by compacting 10 mg of CeO_2@UiO-66-$(SH)_2$ into a glass column and subsequently capping the column with cotton wool. Afterwards, 5 mL of Milli-Q water was passed through the column. For comparative adsorption, 30 mL of a solution containing 100 ppb each of As(III and V), Cd(II), Cr(III and VI), Cu(II), Pb(II) and Hg(II) was passed through the column at a flow rate of 1.3 mL/min. The filtered metal solution was collected and analyzed by ICP-OES. The adsorption-desorption cycling experiments comprised an *adsorption step*, whereby 30 mL of a solution (pH 5) containing 100 ppb each of As(III), As(V), Cd(II), Cr(III), Cr(VI), Cu(II), Pb(II) and Hg(II) ions was filtered through the column; and a *desorption step*, in which 100 mL of a 250 mM solution of NaH_2PO_4[38] (pH 5) was passed through the column. The cycle was repeated ten times and all collected filtrates were analyzed by ICP-OES to follow Hg(II). The breakthrough curve experiment was performed using the same column setup described above. 2340 mL of a 100 ppb Cr(III) solution were passed through the column collecting aliquots at different time intervals, which were then analyzed by ICP-OES.

Synthetic river-water samples

Water samples that recapitulated the Buringanga River and the Bone River were separately prepared based on reported values (ppb) of metal pollutants in each river.[39,40] Briefly, Milli-Q water solutions containing the necessary metal ions was prepared at both pH 5 and at the natural pH of each river: pH 6.6 (using HNO_3) for the Buringanga River and pH 7.5 (using NaOH) for the Bone River. The solutions were stored at 4 ˚C in the dark until use.

River-water metal adsorption

Similarly to in the adsorption procedures described above, 1 mg of CeO_2@UiO-66-$(SH)_2$ was loaded into 50 mL Falcon centrifugation tubes containing 30 mL samples (Bone River, Buringanga River or Sarno River), either at pH 5 or at the corresponding natural pH. The rest of the procedure was the same as for the single-metal and multi-metal analyses (see above). The experiment was repeated with 1 mg of CeO_2@UiO-66, but only for the Bone River sample. The samples of the three rivers at their natural pH were also filtered through the packed-powder column prototype. The procedure was the same as for the multiple-pollutant analysis using the column prototype (see above).

Insert figure 1

Magnetically-functionalized adsorption

0.3 mg of CeO_2/Fe_3O_4@UiO-66-$(SH)_2$ was added to an aqueous solution (10 mL, pH 5) containing 100 ppb each of As(III), As(V), Cd(II), Cr(III), Cr(VI), Cu(II), Pb(II) and Hg(II). The suspension was agitated for 3 hours at 30 rpm in a rotary agitator at room temperature. The CeO_2/Fe_3O_4@UiO-66-$(SH)_2$ microbeads were then recovered with a neodymium magnet, and the supernatant was collected through a 200 µm syringe filter and stored at 4 ˚C in the dark until ICP-OES analysis.

Adsorption calculations

In each of the adsorption tests, the maximum uptake capacity (L_M) of the microbeads was calculated as:

$$L_M = \frac{C_0 \times V}{M}$$

where C_0 is the initial concentration of the solution; V, the volume loaded into the Falcon tube; and M, the mass of MOF used for the adsorption.

The pollutant-loading level (L) of the microbeads was calculated as:

$$L = \frac{(C_0 - C_f) \times V}{M}$$

, where C_f is the final measured concentration.

And finally, the percentage of pollutant adsorbed from each sample was calculated as follows:

$$\%Adsorption = \frac{L}{L_M} \times 100$$

RESULTS AND DISCUSSION

Synthesis and characterization

The UiO-66 and CeO_2@UiO-66 microbeads, and their corresponding thiol-functionalized derivatives UiO-66-$(SH)_2$ and CeO_2@UiO-66-$(SH)_2$, were synthesized following a continuous-flow spray-drying methodology previously reported by our group (Fig. 1a).[37,41] In a typical synthesis, a solution containing the corresponding MOF precursors and dispersed CeO_2 NPs (for the composites) were injected into a coil-flow reactor and subsequently spray-dried, leading to the formation of dense microscale beads in the form of dry powders.

FE-SEM of all four samples revealed the formation of spherical beads (average size: 1.5 µm ± 1.0 µm) formed by nanocrystals of UiO-66 and UiO-66-$(SH)_2$ (Fig. 1b). X-ray powder diffraction (XRPD) on the beads revealed a pure, crystalline, UiO-66-type framework (Fig. S2). Moreover, high-angle annular dark-field scanning transmission electron microscopy (HAADF-STEM) on CeO_2@UiO-66 and on CeO_2@UiO-66-$(SH)_2$ confirmed the encapsulation of disperse CeO_2 NPs inside them (Fig. 1b). The

samples were digested with 5% HF, and the supernatant was filtered, and then used for quantification of the CeO_2 iNP content by ICP-OES. The iNP-content values found were 4.0% (w/w) for CeO_2@UiO-66 (encapsulation yield: 93%) and 3.3% (w/w) for CeO_2@UiO-66-$(SH)_2$ (encapsulation yield: 87%).

The porosity of all four samples was confirmed by nitrogen adsorption analysis at 77 K, from which the following BET surface areas were found: 945 m^2/g (UiO-66), 597 m^2/g (UiO-66-$(SH)_2$), 747 m^2/g (CeO_2@UiO-66) and 539 m^2/g (CeO_2@UiO-66-$(SH)_2$) (Fig. S3). The values for the pristine MOFs are consistent with literature reports.[42] The collected isotherms were found to be type IV (IUPAC classification) isotherms presenting hysteresis loops. This behavior is typical of MOF beads made by spray-drying and can be attributed to the presence of some mesoporosity derived from the nanocrystal assembly that forms the beads.

Metal-adsorption capacity

We evaluated the potential of our microbeads as adsorbents for the most prevalent heavy-metal pollutants in industrial wastewater: As(III and V), Cd(II), Cr(III and VI), Cu(II), Pb(II) and Hg(II). To this end, each sample (bead concentration: 0.03 mg/mL) was incubated in aqueous solutions (pH 5) of the different metal ions (100 ppb) for 3 hours under continuous stirring. Note that the pH of the aqueous solutions was fixed at 5 to prevent precipitation of the metal ions during the adsorption studies. The metal-ion concentration of 100 ppb was selected because it falls within the range of concentrations for metal ions found in contaminated waters (see, for example Table 1). After 3 hours, the beads were separated from the aqueous solutions and the amount of metal ions remaining in the supernatants was evaluated by ICP-OES.

The adsorption capacity values for all metal ions are shown in Figure 2a and Table S1, revealing two clear trends. Firstly, the pendant thiol groups confer a functional benefit: in all cases, relative to UiO-66, the UiO-66-$(SH)_2$ demonstrated superior uptake of all the metal ions except As(V). The anomaly for As(V) uptake can be rationalized according to its distinct adsorption mechanism, in which the ions are adsorbed by the zirconium clusters through Zr-O-As coordination bonds,[10,22] which are more easily accessible without the steric hindrance of the thiol groups. The second trend is that incorporation of CeO_2 NPs into MOF microbeads enhances adsorption of both As(III) and Cr(IV), as expected from the previously reported activity and selectivity of these NPs towards these metal ions.[25,43] This functional gain is important, as As(III) and Cr(IV) are highly toxic pollutants and, especially in the case of the latter, exhibit high mobility,[4,44] making them a high priority for removal from industrial wastewater. Moreover, compared to the case of other metals, efficient removal of these two metal ions from water usually takes longer, suffers from lower uptakes and requires a previous chemical conversion.[45]

Insert figure 2

Altogether, our results prompted us to select CeO_2@UiO-66-$(SH)_2$ for a test of simultaneous adsorption of all the metals. To this end, CeO_2@UiO-66-$(SH)_2$microbeads were incubated in an aqueous mixture containing all the aforementioned metal ions at a concentration of 100 ppb each (Fig. 2b). The CeO_2@UiO-66-$(SH)_2$ microbeads removed 99 ppb Pb(II) (99%), 99 ppb Cu(II) (99%), 98 ppb Hg(II) (98%), 185 ppb Cr(III and VI) (93%), 87 ppb Cd(II) (87%), 111 ppb As(III and V) (56%). Thus, CeO_2@UiO-66-$(SH)_2$ simultaneously captured all the different metal ions while demonstrating the same adsorption capacity for each one as in the previous single-metal adsorption experiments.

In addition to strongly adsorbing target pollutants from water, MOF-based adsorbents must also be stable and not release their component metal ions (in our case, Zr(IV) plus Ce(IV), to form the MOF and the iNP) into the water. Accordingly, we also investigated the presence of these metal ions in the aqueous solutions of the adsorption experiments. Zr(IV) and Ce(IV) were not detected in any of the samples, confirming the stability of the microbeads. Moreover, and further confirming the stability of the microbeads, XRPD after the metal-adsorption experiments indicated that all the microbeads had retained the crystallinity of the parent samples (Fig. S2).

iNP@MOF -Beads as packing material in a column for continuous-flow removal of metals from water

Once we had demonstrated that our microbeads effectively remove heavy metal ions from water, we next evaluated their performance as packing material in a purification column. To this end, 10 mg of CeO_2@UiO-66-$(SH)_2$ were packed into a 5 mm-diameter glass column (Fig. 3a), through which 30 mL of an aqueous solution (pH 5) of As(III), As(V), Cd(II), Cr(III), Cr(VI), Cu(II), Pb(II) and Hg(II) (100 ppb each) was passed through at a flow rate of 1.3 mL/min. The filtrate was analyzed by ICP-OES, revealing the following removal rates for each metal: Pb(II) (99%); Hg(II) (99%); Cu(II) (99%); Cd(II) (85%); Cr(III and VI) (84%); As(III and V) (69%) (Fig. 3b). Thus, after purification by the microbeads, the final remaining concentration of each metal in the water sample was: Pb(II) and Hg(II) (less than 0.25 ppb); Cu(II) (0.3 ppb); Cd(II) (15 ppb); Cr(III and VI) (32 ppb); and As(III and V) (62 ppb). Remarkably, the concentration of all metals in the water sample could be reduced down to 0.25 ppb by passing this latter sample twice more through the column (Fig. 3b). In addition, using Cr(III) as a model metal ion, we performed a breakthrough curve with a 10 mg packed powder bed of CeO_2@UiO-66-$(SH)_2$, a feed solution with a Cr(III) concentration of 100 ppb, and a flow rate of 1.3 mL/min (Fig. S4). From the obtained data, we could determine a breakthrough time (10%C_0) of 231 minutes (300.6 mL) and an exhaust time (90%C_0) of 1239 minutes (1610.4 mL). The degree of saturation was calculated to be 45%,[46] and the maximum loading capacity of the column was 82.7 mg of Cr(III) per g of adsorbent. This capture capacity value compares favorably with other fixed bed adsorption studies found in the literature.[47]

Insert figure 3

An important aspect to be considered when using a new adsorbent in packed columns is its regeneration, which in our case, corresponds to metal-ion desorption from CeO_2@UiO-66-$(SH)_2$. To explore this property, we tested the CeO_2@UiO-66-$(SH)_2$-packed column over three adsorption/desorption cycles. The adsorption step comprised filtering 30 mL of an aqueous solution (pH 5) of all the studied metals (100 ppb each).The desorption (regeneration) step entailed passing 100 mL of a 250 mM aqueous solution of $H_2PO_4^-$ (pH 5) through the column at a flow rate of 1.3 mL/min. ICP-OES analysis of the collected filtrate revealed almost complete desorption (>96%) and recovery of most the metal ions (As(III and V), Cd(II), Cr(III and VI, Cu(II) and Pb(II))) and high desorption (>91%) and recovery of Hg(II) (Fig. 4a,b). To further demonstrate the regeneration of CeO_2@UiO-66-$(SH)_2$, this adsorption/desorption cycle was repeated ten times and all the collected filtrates were analyzed by ICP-OES to determine the desorption of Hg^{2+}. Interestingly, the corresponding uptake rates were similar among the ten cycles, meaning that the regeneration process was sufficient to maintain the adsorption capacity of our microbeads (Fig. 4b).

Insert figure 4

Metal removal in synthetic and real river-water samples

Having preliminarily demonstrated the metal-adsorption capacities of our microbeads, we next evaluated them in test cases corresponding to known cases of river pollution. Firstly, synthetic river-water samples were prepared to independently recapitulate the Buringanga River[39] (Bangladesh) and the Bone River[40] (Indonesia), both of which contain metal ions at concentrations well-above the WHO standards (Table 1). Specifically, the Buringanga River is contaminated with Cd(II), Cr(III), Cu(II) and Pb(II), whereas the Bone River is contaminated with Hg(II), As(V) and Pb(II). Initially, CeO_2@UiO-66-$(SH)_2$ microbeads (bead concentration: 0.03 mg/mL) were incubated in the synthetic samples for 3 hours under continuous stirring. Then, the microbeads were separated from the water samples and the concentration of metal ions remaining in the treated water river samples was determined by ICP-OES. Note that the adsorption was tested at the natural pH of each river (pH 6.6 for the Buringanga River and pH 7.5 for the Bone River) as well as at pH 5, for comparison. Table 1 shows the heavy-metal ion capture capacity of the CeO_2@UiO-66-$(SH)_2$ microbeads.

Insert table 1

For the Buringanga River sample at pH 6.6, the microbeads removed more than 98% of Cd(II), Cu(II) and Pb(II) ions and 69% of Cr(III) ions; thus, the microbeads had reduced the concentration of each metal to below the WHO limits (Table 1). At pH 5, the microbeads exhibited slightly different performance, adsorbing more than 98% of the Cr(III), Cu(II) and Pb(II) ions, while removing only 65% of the Cd(II) (Table 1). Consequently, the remaining concentration of Cd(II) in the supernatant (23 ppb) was above the corresponding WHO limit.

For the Bone River sample at pH 5, the CeO_2@UiO-66-$(SH)_2$ microbeads captured more than 99% of Hg(II) and Pb(II), leaving behind only 2.5 ppb and 1.4 ppb, respectively both under the WHO limits. However, it could not efficiently capture As(V), leaving behind 109 ppb, which is well above the corresponding WHO limit. At Bone's natural pH 7.5, the CeO_2@UiO-66-$(SH)_2$ microbeads adsorbed 99% of Pb(II) and 31 % As(V), which is still above the WHO limit. Fortunately, UiO-66@CeO_2 microbeads adsorbed 62% of the As(V), leaving behind 46 ppb of the latter, which, while above the WHO limit, is below the water standards concentration for Indonesia (Table 1). Note that the adsorption of Hg(II) at pH 7.5 could not be analyzed, as Hg(II) begins to precipitate out at pH 6 and above. At such pH values, the Hg(II) precipitates are typically removed by filtration or flocculation systems.

To evaluate our CeO_2@UiO-66-$(SH)_2$ microbeads for purification of real field samples from rivers, we also tested them for removal of metals from a sample collected from the Sarno River, in Italy (pH 7.2). Although the Sarno River currently meets the WHO standards for metal-ion levels in potable water, its Cr(VI) levels presently exceed those of other European rivers. The Sarno River sample contained 11 ppb of Cr(VI) and minuscule amounts of As(III) (0.9 ppb) and Cu(II) (3.2 ppb), of which the CeO_2@UiO-66-$(SH)_2$ microbeads captured 37%, 55% and 99%, respectively (Table 1).

Next, we studied the continuous-flow removal of metals from the three river samples using the column containing packed CeO_2@UiO-66-$(SH)_2$ microbeads (10 mg). To this end, 30 mL of each river sample was passed through the column at a flow rate of 1.3 mL/min. For the Buringanga River sample, the column removed more than 99% of Cd(II), Cu(II) and Pb(II) ions and 90% of Cr(III) ions; and for the Bone River sample, it adsorbed 99% of the Pb(II) and 86% of the As(V). In both cases, purification through the column reduced the concentration of each metal to below the WHO limits (Table 1). In the case of the Sarno River sample, the column removed 99% of all Cr(VI), As(III) and Cu(II).

Magnetically functionalized iNP@MOF-Beads

Finally, having demonstrated that our microbeads can remove various heavy metals from water, we sought to explore the possibility of conferring them with magnetism, such they could be magnetically removed after water purification. To this end, we turned again to spray-drying, which can be exploited to incorporate multiple classes of nanoparticles into MOF microbeads. Thus, CeO_2 and Fe_3O_4 NPs were simultaneously incorporated into UiO-66-$(SH)_2$ to afford a magnetically responsive microbead, CeO_2/Fe_3O_4@UiO-66-$(SH)_2$ (Fig. 5a). FE-SEM and XRPD confirmed the formation of spherical microbeads built of UiO-66-$(SH)_2$ nanocrystals (Fig. 5b and Fig. S5). Furthermore, HAADF-STEM, EDX and ICP-OES analyses revealed successful incorporation of both types of iNPs into the composite microbeads at the following content levels (w/w): 3.0% for CeO_2 and 9.3% for Fe_3O_4 (Fig. 5b and Fig. S6).

Insert figure 5

We then tested the adsorption capacity of the CeO_2/Fe_3O_4@UiO-66-$(SH)_2$ microbeads by incubating (0.03 mg/mL) them in a water sample containing 100 ppb each of As(III), As(V), Cd(II), Cr(III), Cr(VI), Cu(II), Pb(II) and Hg(II), under continuous stirring. After 3 hours, the microbeads were separated out from the water sample by approaching a neodymium magnet to the water sample for 5 minutes (Fig. 5c), and the amount of metal ions remaining in the treated water sample was evaluated by ICP-OES. Remarkably, the microbeads showed comparable metal-ion adsorption capacity to that of the original non-magnetic microbeads, CeO_2@UiO-66-$(SH)_2$ (Fig. 5d).

CONCLUSIONS

We have designed, developed and tested iNP@MOF composite microbeads as adsorbents for removal of heavy metal ions from water. The spherical microbeads are formed in one step by continuous-flow spray-drying. They efficiently and simultaneously remove various metal ions from water, including As(III and V), Cd(II), Cr(III and VI), Cu(II), Pb(II) and Hg(II), are stable during water purification, and can be regenerated by a gentle acidic treatment. We also successfully evaluated the best-performing of these microbeads, UiO-66-$(SH)_2$@CeO_2, as packing material in a continuous-flow column for water purification. We further confirmed the efficiency of CeO2@UiO-66-(SH)2 by testing it in synthetic and real river-water samples. For the samples that recapitulated the Bone River and the Buringanga River, treatment with our microbeads reduced the levels of most of the harmful metals to below the WHO limits; and for the Sarno River sample, it significantly reduced the relatively high content of Cr(VI). Finally, we explored the idea of conferring our microbeads with magnetism. Harnessing the versatility of spray-drying, we simultaneously incorporated two types of iNPs, CeO_2 and Fe_3O_4, into UiO-66-$(SH)_2$ to obtain CeO_2/Fe_3O_4@UiO-66-$(SH)_2$. The resultant magnetic microbeads demonstrate similar metal-adsorption capacity to the original non-magnetic microbeads and can easily be removed from treated

water by a magnet. Given their ready formation and tunability, we are confident that such iNP@MOF-Beads will prove utile in future water-purification applications.

ASSOCIATED CONTENT

Supporting information

The supporting information is available free of charge on the ACS Publications website at DOI: 10.1021/acsami.0x00000.

Additional figures include H-NMR spectra of the synthetized ligand; XRPD spectra of the studied materials; BET analysis of the studied materials; Table of the removal efficiency for single pollutant experiments; XRPD of the magnetic composite material; EDX analysis of the magnetic composite material

Author information

Corresponding author

*E-mail: daniel.maspoch@icn2.cat, inhar.imaz@icn2.cat

ORCID

Daniel Maspoch: 0000-0003-1325-9161
Inhar Imaz: 0000-0002-0278-1141

Notes

The authors declare no competing financial interest.

ACKNOWLEDGEMENTS

This work was supported by the Spanish MINECO (project RTI2018-095622-B-I00), the Catalan AGAUR (project 2017 SGR 238), and the ERC, under the EU-FP7 (ERC-Co 615954). It was also funded by the CERCA Program/Generalitat de Catalunya. ICN2 is supported by the Severo Ochoa program from the Spanish MINECO (Grant No. SEV-2017-0706).

REFERENCES

(1) Bakker, K. Water Security: Research Challenges and Opportunities. *Science* **2012**, *337*, 914 - 915.

(2) Dos Santos, C. E.; Dal Pizzol, V. I.; Aragão, S. C.; Filho, A. R.; Marques, F. M. Vasculite c-ANCA Relacionada Em Paciente Com Retocolite Ulcerativa: Relato de Caso. *Rev. Bras. Reumatol.* **2013**, *53* 441–443.

(3) Gleick, P. H. Global Freshwater Resources: Soft-Path Solutions for the 21st Century. *Science* **2003**, *302* 1524–1528.

(4) Tchounwou, P. B.; Yedjou, C. G.; Patlolla, A. K.; Sutton, D. J. Molecular, Clinical and Environmental Toxicology. **2012**, *101*, 1–30.

(5) WHO. Guidelines for Drinking-Water Quality: Incorporating 1st and 2nd Addenda, Vol. 1, Reccomendations - 3rd Edition. *WHO Chron.* **2008**, *38*, 668.

(6) Jaishankar, M.; Tseten, T.; Anbalagan, N.; Mathew, B. B.; Beeregowda, K. N. Toxicity, Mechanism and Health Effects of Some Heavy Metals. *Interdiscip. Toxicol.* **2014**, *7*, 60–72.

(7) Li, B.; Zhang, Y.; Ma, D.; Shi, Z.; Ma, S. Mercury Nano-Trap for Effective and Efficient Removal of mercury(II) from Aqueous Solution. *Nat. Commun.* **2014**, *5*, 1–7.

(8) Huang, N.; Zhai, L.; Xu, H.; Jiang, D. Stable Covalent Organic Frameworks for Exceptional Mercury Removal from Aqueous Solutions. *J. Am. Chem. Soc.* **2017**, *139*, 2428–2434.

(9) Liu, B.; Jian, M.; Liu, R.; Yao, J.; Zhang, X. Highly Efficient Removal of arsenic(III) from Aqueous Solution by Zeolitic Imidazolate Frameworks with Different Morphology. *Colloids Surfaces A Physicochem. Eng. Asp.* **2015**, *481*, 358–366.

(10) Wang, C.; Liu, X.; Chen, J. P.; Li, K. Superior Removal of Arsenic from Water with Zirconium Metal-Organic Framework UiO-66. *Sci. Rep.* **2015**, *5*, 1–10.

(11) Kumar, P.; Pournara, A.; Kim, K. H.; Bansal, V.; Rapti, S.; Manos, M. J. Metal-Organic Frameworks: Challenges and Opportunities for Ion-Exchange/sorption Applications. *Prog. Mater. Sci.* **2017**, *86*, 25–74.

(12) Hlongwane, G. N.; Sekoai, P. T.; Meyyappan, M.; Moothi, K. Simultaneous Removal of Pollutants from Water Using Nanoparticles: A Shift from Single Pollutant Control to Multiple Pollutant Control. *Sci. Total Environ.* **2019**, *656*, 808–833.

(13) Mon, M.; Bruno, R.; Ferrando-Soria, J.; Armentano, D.; Pardo, E. Metal-Organic Framework Technologies for Water Remediation: Towards a Sustainable Ecosystem. *Journal of Materials Chemistry A*. **2018**, 6, 4912–4947.

(14) Kobielska, P. A.; Howarth, A. J.; Farha, O. K.; Nayak, S. Metal–organic Frameworks for Heavy Metal Removal from Water. *Coord. Chem. Rev.* **2018**, *358*, 92–107.

(15) Dhaka, S.; Kumar, R.; Deep, A.; Kurade, M. B.; Ji, S. W.; Jeon, B. H. Metal–organic Frameworks (MOFs) for the Removal of Emerging Contaminants from Aquatic Environments. *Coord. Chem. Rev.* **2019**, *380*, 330–352.

(16) Gao, Q.; Xu, J.; Bu, X. H. Recent Advances about Metal–organic Frameworks in the Removal of Pollutants from Wastewater. *Coord. Chem. Rev.* **2019**, *378*, 17–31.

(17) Wen, J.; Fang, Y.; Zeng, G. Progress and Prospect of Adsorptive Removal of Heavy Metal Ions from Aqueous Solution Using Metal–organic Frameworks: A Review of Studies from the Last Decade. *Chemosphere* **2018**, *201*, 627–643.

(18) Mon, M.; Bruno, R.; Tiburcio, E.; Viciano-Chumillas, M.; Kalinke, L. H. G.; Ferrando-Soria, J.; Armentano, D.; Pardo, E. Multivariate Metal–Organic Frameworks for the Simultaneous Capture of Organic and Inorganic Contaminants from Water. *J. Am. Chem. Soc.* **2019**, *141*, 13601–13609.

(19) Noraee, Z.; Jafari, A.; Ghaderpoori, M.; Kamarehie, B.; Ghaderpoury, A. Use of Metal-Organic Framework to Remove Chromium (VI) from Aqueous Solutions. *J. Environ. Heal. Sci. Eng.* **2019**, 1–9.

(20) Saleem, H.; Rafique, U.; Davies, R. P. Investigations on Post-Synthetically Modified UiO-66-NH2 for the Adsorptive Removal of Heavy Metal Ions from Aqueous Solution. *Microporous Mesoporous Mater.* **2016**, *221*, 238–244.

(21) Yee, K. K.; Reimer, N.; Liu, J.; Cheng, S. Y.; Yiu, S. M.; Weber, J.; Stock, N.; Xu, Z. Effective Mercury Sorption by Thiol-Laced Metal-Organic Frameworks: In Strong Acid and the Vapor Phase. *J. Am. Chem. Soc.* **2013**, *135*, 7795–7798.

(22) Audu, C. O.; Nguyen, H. G. T.; Chang, C. Y.; Katz, M. J.; Mao, L.; Farha, O. K.; Hupp, J. T.; Nguyen, S. T. The Dual Capture of As V and As III by UiO-66 and Analogues. *Chem. Sci.* **2016**, *7*, 6492–6498.

(23) Simeonidis, K.; Mourdikoudis, S.; Kaprara, E.; Mitrakas, M.; Polavarapu, L. Inorganic Engineered Nanoparticles in Drinking Water Treatment: A Critical Review. *Environ. Sci. Water Res. Technol.* **2016**, *2*, 43–70.

(24) Prasse, C.; Ternes, T. Removal of Organic and Inorganic Pollutants and Pathogens from Wastewater and Drinking Water Using Nanoparticles - A Review. *Nanoparticles in the Water Cycle: Properties, Analysis and Environmental Relevance*; Springer Berlin Heidelberg, **2010**; 55–79.

(25) Feng, Q.; Zhang, Z.; Ma, Y.; He, X.; Zhao, Y.; Chai, Z. Adsorption and Desorption Characteristics of Arsenic onto Ceria Nanoparticles. *Nanoscale Res. Lett.* **2012**, *7*, 1–8.

(26) Recillas, S.; Colón, J.; Casals, E.; González, E.; Puntes, V.; Sánchez, A.; Font, X. Chromium VI Adsorption on Cerium Oxide Nanoparticles and Morphology Changes during the Process. *J. Hazard. Mater.* **2010**, *184*, 425–431.

(27) Contreras, A. R.; Casals, E.; Puntes, V.; Komilis, D.; Sánchez, A.; Font, X. Use of Cerium Oxide (CeO2) Nanoparticles for the Adsorption of Dissolved Cadmium (II), Lead (II) and Chromium (VI) at Two Different pHs in Single and Multi-Component Systems. *Glob. Nest J.* **2015**, *17* , 536–543.

(28) Olivera, S.; Chaitra, K.; Venkatesh, K.; Muralidhara, H. B.; Inamuddin; Asiri, A. M.; Ahamed, M. I. Cerium Dioxide and Composites for the Removal of Toxic Metal Ions. *Environ. Chem. Lett.* **2018**, *16*, 1233–1246.

(29) Falcaro, P.; Ricco, R.; Yazdi, A.; Imaz, I.; Furukawa, S.; Maspoch, D.; Ameloot, R.; Evans, J. D.; Doonan, C. J. Application of Metal and Metal Oxide Nanoparticles at MOFs. *Coord. Chem. Rev.* **2016**, *307*, 237–254.

(30) Zhao, G.; Qin, N.; Pan, A.; Wu, X.; Peng, C.; Ke, F.; Iqbal, M.; Ramachandraiah, K.; Zhu, J. Magnetic Nanoparticles@Metal-Organic Framework Composites as Sustainable Environment Adsorbents. *J. Nanomater.* **2019**, *2019*, 1–11.

(31) Sivashankar, R.; Sathya, A. B.; Vasantharaj, K.; Sivasubramanian, V. Magnetic Composite an Environmental Super Adsorbent for Dye Sequestration - A Review. *Environ. Nanotechnology, Monit. Manag.* **2014**, *1–2*, 36–49.

(32) Bedia, J.; Muelas-Ramos, V.; Peñas-Garzón, M.; Gómez-Avilés, A.; Rodríguez, J. J.; Belver, C. A Review on the Synthesis and Characterization of Metal Organic Frameworks for Photocatalytic Water Purification. *Catalysts* **2019**, *9*, 52.

(33) Santhosh, C.; Malathi, A.; Daneshvar, E.; Kollu, P.; Bhatnagar, A. Photocatalytic Degradation of Toxic Aquatic Pollutants by Novel Magnetic 3D-TiO2@HPGA Nanocomposite. *Sci. Rep.* **2018**, *8*, 1–15.

(34) Vial, L.; Ludlow, R. F.; Leclaire, J.; Pérez-Fernández, R.; Otto, S. Controlling the Biological Effects of Spermine Using a Synthetic Receptor. *J. Am. Chem. Soc.* **2006**, *128* , 10253–10257.

(35) Zhang, F.; Jin, Q.; Chan, S.-W. Ceria Nanoparticles: Size, Size Distribution, and Shape. *J. Appl. Phys.* **2004**, *95*, 4319–4326.

(36) Zhang, F.; Chan, S. W.; Spanier, J. E.; Apak, E.; Jin, Q.; Robinson, R. D.; Herman, I. P. Cerium Oxide Nanoparticles: Size-Selective Formation and Structure Analysis. *Appl. Phys. Lett.* **2002**, *80*, 127–129.

(37) Yazdi, A.; Abo Markeb, A.; Garzón-Tovar, L.; Patarroyo, J.; Moral-Vico, J.; Alonso, A.; Sánchez, A.; Bastus, N.; Imaz, I.; Font, X.; Puntes, V; Maspoch, D. Core-Shell Au/CeO2 Nanoparticles Supported in UiO-66 Beads Exhibiting Full CO Conversion at 100 °c. *J. Mater. Chem. A* **2017**, *5*, 13966–13970.

(38) Folens, K.; Leus, K.; Nicomel, N. R.; Meledina, M.; Turner, S.; Van Tendeloo, G.; Laing, G. Du; Van Der Voort, P. Fe3O4@MIL-101 – A Selective and Regenerable Adsorbent for the Removal of As Species from Water. *Eur. J. Inorg. Chem.* **2016**, *2016*, 4395–4401.

(39) Bhuiyan, M. A. H.; Dampare, S. B.; Islam, M. A.; Suzuki, S. Source Apportionment and Pollution Evaluation of Heavy Metals in Water and Sediments of Buriganga River, Bangladesh, Using Multivariate Analysis and Pollution Evaluation Indices. *Environ. Monit. Assess.* **2015**, *187*.

(40) Gafur, N. A.; Sakakibara, M.; Sano, S.; Sera, K. A Case Study of Heavy Metal Pollution in Water of Bone River by Artisanal Small-Scale Gold Mine Activities in Eastern Part of Gorontalo, Indonesia. *Water (Switzerland)* **2018**, *10* , 1–10.

(41) Garzón-Tovar, L.; Cano-Sarabia, M.; Carné-Sánchez, A.; Carbonell, C.; Imaz, I.; Maspoch, D. A Spray-Drying Continuous-Flow Method for Simultaneous Synthesis and Shaping of Microspherical High Nuclearity MOF Beads. *React. Chem. Eng.* **2016**, *1*, 533–539.

(42) Leus, K.; Perez, J. P. H.; Folens, K.; Meledina, M.; Van Tendeloo, G.; Du Laing, G.; Van Der Voort, P. UiO-66-(SH)2 as Stable, Selective and Regenerable Adsorbent for the Removal of Mercury from Water under Environmentally-Relevant Conditions. *Faraday Discuss.* **2017**, *201*, 145–161.

(43) Xiao, H.; Ai, Z.; Zhang, L. Nonaqueous Sol-Gel Synthesized Hierarchical CeO2 Nanocrystal Microspheres as Novel Adsorbents for Wastewater Treatment. *J. Phys. Chem. C* **2009**, *113*, 16625–16630.

(44) Marinho, B. A.; Cristóvão, R. O.; Boaventura, R. A. R.; Vilar, V. J. P. As(III) and Cr(VI) Oxyanion Removal from Water by Advanced Oxidation/reduction Processes—a Review. *Environ. Sci. Pollut. Res.* **2019**, *26*, 2203–2227.

(45) Sun, M.; Zhang, G.; Qin, Y.; Cao, M.; Liu, Y.; Li, J.; Qu, J.; Liu, H. Redox Conversion of Chromium(VI) and Arsenic(III) with the Intermediates of Chromium(V) and Arsenic(IV) via AuPd/CNTs Electrocatalysis in Acid Aqueous Solution. *Environ. Sci. Technol.* **2015**, *49*, 9289–9297.

(46) Thilagan, J.; Kumar, A. V.; Rajasekaran, K.; Raja, C. Continuous Fixed Bed Column Adsorption of the Copper(II) Ions from Aqueous Solution by Calcium Carbonate *Int. J. Res. Eng. Technol.* **2015**, 4, 413-418

(47) Patel, H. Fixed-bed column adsorption study: a comprehensive review. *Appl. Water Sci.* **2019**, 9, 45.

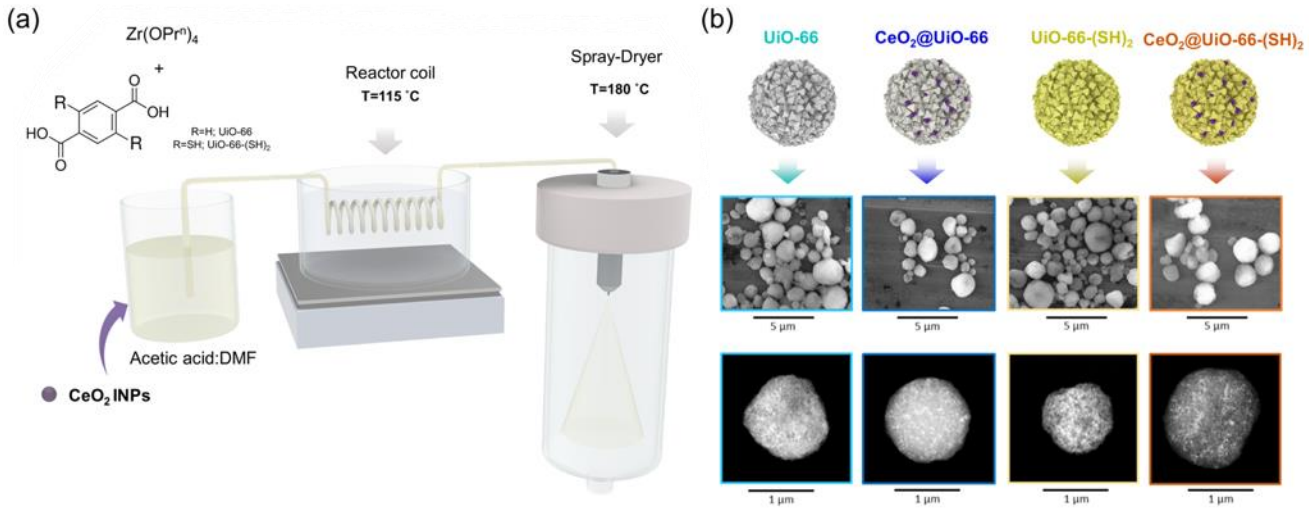

Fig. 1. a) Schematic of the continuous-flow spray-drying synthesis of MOF microbeads and iNP@MOF-Beads. b) Schematic (top), FE-SEM images (medium) and HAADF-STEM images (bottom) of MOF microbeads and iNP@MOF-Beads.

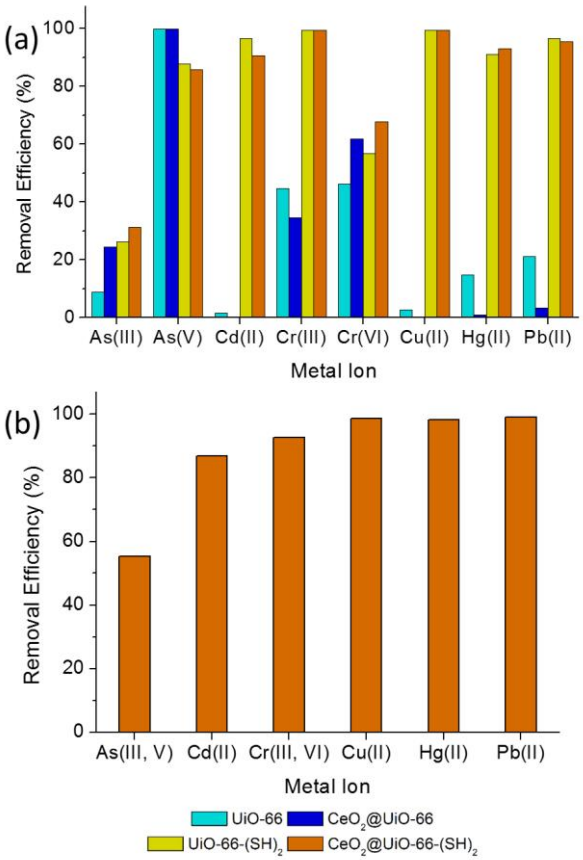

Fig. 2. a) Single-metal removal efficiency for UiO-66 (cyan), CeO_2@UiO-66 (blue), UiO-66$(SH)_2$ (yellow) and CeO_2@UiO-66-$(SH)_2$ (orange). b) Multiple-metal removal efficiency for CeO_2@UiO-66-$(SH)_2$.

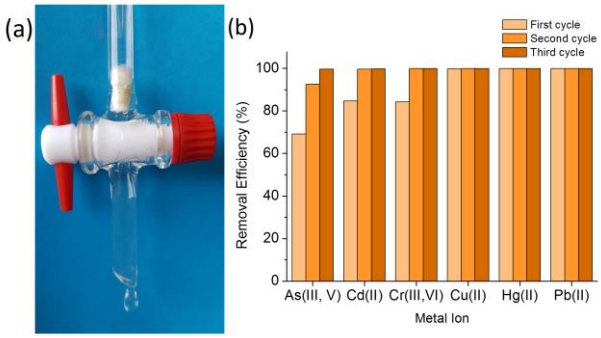

Fig. 3. a) Photograph of the continuous-flow column setup. b) Multiple- metal removal efficiency for the column containing CeO_2@UiO-66-$(SH)_2$ as packing material. In this experiment, an aqueous solution (pH 5) of As(III), As(V), Cd(II), Cr(III), Cr(VI), Cu(II), Pb(II) and Hg(II) (100 ppb each) was passed through the column three times.

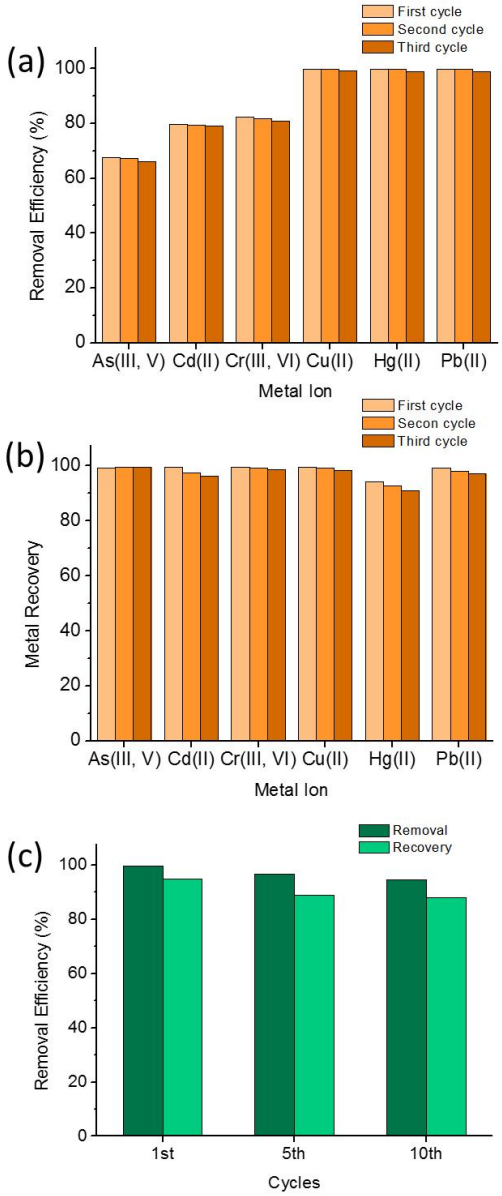

Fig. 4. (a,b) Multiple-metal removal efficiency (a) and recovery (b, regeneration) for the column after three adsorption/desorption cycles. (c) Hg(II) removal efficiency and recovery (regeneration) for the column after ten cycles of sequential adsorption/desorption steps. The adsorption step comprised passing through the column, 10 mL of water containing each metal-ion pollutant (100 ppb). The desorption step comprised passing through the column, 100 mL of 250 mM aq. $H_2PO_4^-$ (pH = 5).

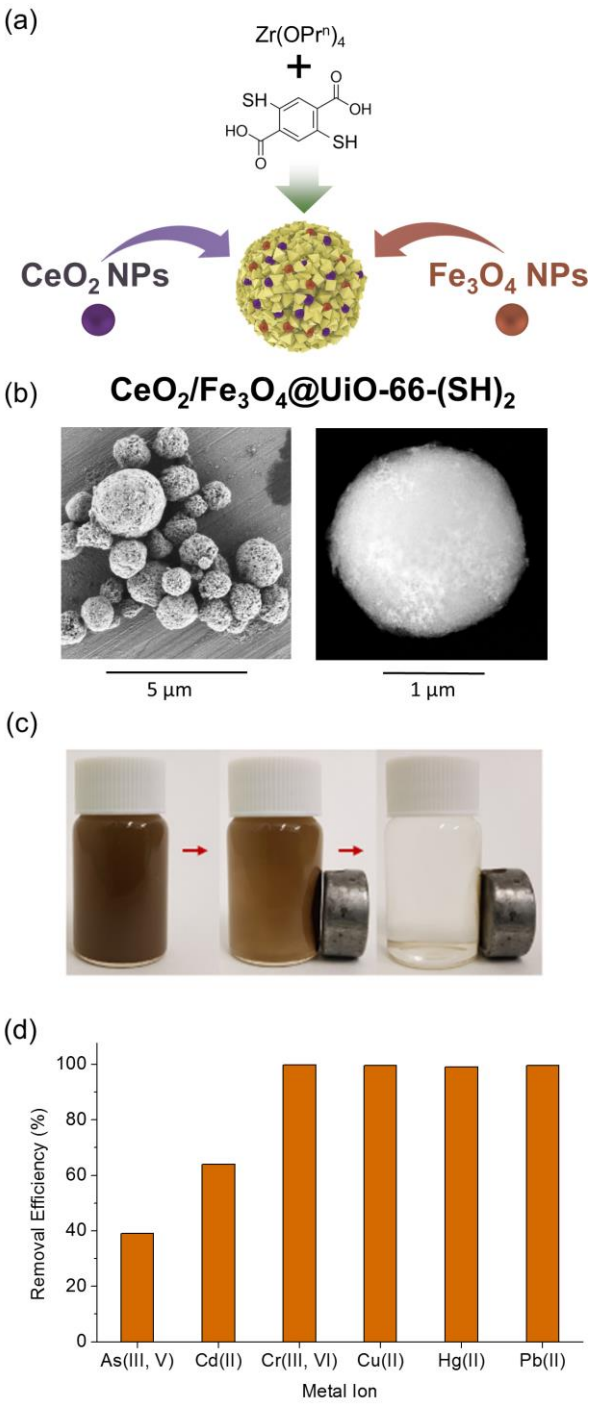

Fig. 5. a) Schematic of the synthesis of CeO_2/Fe_3O_4@UiO-66-$(SH)_2$. b) FE-SEM images (left) and HAADF-STEM images (right) of CeO_2/Fe_3O_4@UiO-66-$(SH)_2$. c) Photograph of a dispersion of CeO_2/Fe_3O_4 @UiO-66-$(SH)_2$ microbeads before (left) and after (middle) approach of a neodymium magnet, and after complete magnetic recovery (5 minutes in contact with the magnet; right). d) Multiple-metal removal efficiency for magnetically-recovered CeO_2/Fe_3O_4@UiO-66-$(SH)_2$.

Table 1. Results of metal-adsorption experiments (at pH = 5 and at the natural pH for each river), showing the maximum heavy-metal concentration permitted by WHO standards. The values marked with "*" correspond to adsorption by CeO_2@UiO-66.

Buringanga

	Adsorption pH = 5			Adsorption pH = 6,6			Continuous flow pH = 6,6			
Metal pollutant	Before (ppb)	After (ppb)	Removed (%)	Before (ppb)	After (ppb)	Removed (%)	Before (ppb)	After (ppb)	Removed (%)	WHO standards (ppb)
Cd(II)	67	23	65%	66	1.3	98%	66	0.3	99%	3
Cr(III)	114	1.1	99%	105	33	69%	105	11	90%	50
Cu(II)	249	10	96%	243	2.1	99%	243	0.9	99%	2000
Pb(II)	95	< 0.25	99%	98	< 0.25	99%	98	< 0.25	99%	10

Bone

	Adsorption pH = 5			Adsorption pH = 7,5			Continuous-flow pH = 7,5			
Metal pollutant	Before (ppb)	After (ppb)	Removed (%)	Before (ppb)	After (ppb)	Removed (%)	Before (ppb)	After (ppb)	Removed (%)	WHO standards (ppb)
As(V)	122	109	11%	122	84 46*	31% 62%*	122	18	86%	10
Hg(II)	178	2.5	99%	-	-	-	-	-	-	6
Pb(II)	165	1.4	99%	157	1.6	99%	157	4.6	99%	10

Sarno

	Adsorption pH = 5			Adsorption pH = 7,5			Continuous-flow pH = 7,2			
Metal pollutant	Before (ppb)	After (ppb)	Removed (%)	Before (ppb)	After (ppb)	Removed (%)	Before (ppb)	After (ppb)	Removed (%)	WHO standards (ppb)
As(III)	0.9	0.5	45%	0.9	0.4	55%	0.9	< 0.25	99%	10
Cr(VI)	11	7.7	30%	11	6.9	37%	11	< 0.25	99%	50
Cu(II)	3.2	< 0.25	99%	3.2	< 0.25	99%	3.2	< 0.25	99%	2000